Title

EFFECTS OF SILICON ADDITIONS AND RETAINED AUSTENITE ON STRESS CORROSION CRACKING BEHAVIOR OF COMMERCIAL ULTRA-HIGH STRENGTH STEELS IN AQUEOUS SOLUTION

Author

Ritchie, Robert O.

Publication Date

1977-06-01

Submitted to Metallurgical
Transactions A

Preprint

EFFECTS OF SILICON ADDITIONS AND RETAINED AUSTENITE ON STRESS CORROSION CRACKING BEHAVIOR OF COMMERCIAL ULTRA-HIGH STRENGTH STEELS IN AQUEOUS SOLUTION

Robert O. Ritchie, M. H. Castro Cedẽno,
V. F. Zackay, and E. R. Parker

June 1977

Prepared for the U. S. Energy Research and
Development Administration under Contract W-7405-ENG-48

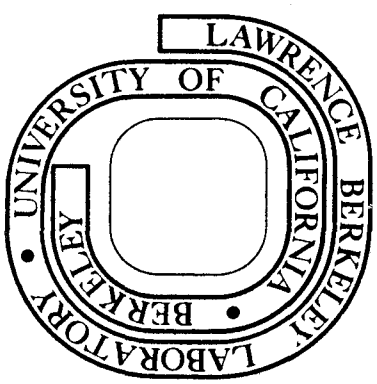

DISCLAIMER

Submitted to Metallurgical Transactions A LBL-5499

COMMUNICATION:

EFFECTS OF SILICON ADDITIONS AND RETAINED AUSTENITE ON STRESS CORROSION CRACKING BEHAVIOR OF COMMERCIAL ULTRA-HIGH STRENGTH STEELS IN AQUEOUS SOLUTION

Robert O. Ritchie, M. H. Castro Cedẽno,
V. F. Zackay and E. R. Parker

Materials and Molecular Research Division, Lawrence Berkeley Laboratory,
and Department of Materials Science and Mineral Engineering,
University of California, Berkeley, California 94720

June 1977

Robert O. Ritchie is Assistant Professor, Department of Mechanical Engineering, Massachusetts Institute of Technology, Cambridge MA 02139. M. H. Castro Cedẽno, V. F. Zackay, and E. R. Parker are graduate student, Professor and Professor respectively, in the Department of Materials Science and Mineral Engineering, University of California, Berkeley, CA 94720.

It has been reported[1,2] that alloying additions of silicon to high strength steels, such as AISI 4340, can improve resistance to hydrogen-assisted cracking and stress corrosion cracking (SCC) in aqueous solutions. Furthermore, it has been suggested[3,4] that the presence of retained austenite within a tempered martensitic structure in such steels might also lead to improved resistance. The purpose of this communication is to report some recent data on these effects by examining the susceptibility to SCC of AISI 4340 and 300-M commercial ultra-high strength steels in distilled water and 3.5 wt pct NaCl solution.

The materials studied were of aircraft-quality (vacuum-arc remelted), of composition (in wt pct) shown below:

	C	Mn	Cr	Ni	Mo	Si	S	P	V	Cu
4340	0.41	0.80	0.79	1.75	0.23	0.26	0.004	0.006	-	0.06
300-M	0.42	0.76	0.76	1.76	0.41	1.59	0.002	0.007	0.10	-

The composition of 300-M is essentially that of 4340 modified with 1.3 pct silicon. The structures investigated were compared after conventional quench and tempering and after isothermal transformation heat-treatments, and are summarized in Table I. Ambient temperature mechanical properties are listed in Table II. SCC tests were performed on fatigue pre-cracked 12.7 mm thick, 1-T compact tension specimens, tested under constant load, and growth rates were continuously monitored using a displacement (clip) gage. Values of K_{Iscc}, the threshold stress intensity, were defined in terms of the maximum stress intensity at which no crack propagation could be detected within 100 hours.

The variation of rates of SCC (da/dt) as a function of instantaneous stress intensity (K) for all structures, tested in distilled water, is shown in Figs. 1 and 2 and relevant data is listed in Table III. The influence of silicon additions to 4340 is illustrated in Fig. 1 where 4340 and 300-M are compared in their respective optimum (and commercially utilized) quenched and tempered conditions, namely 4340 tempered at 200°C and 300-M tempered at 300°C. Despite the increase in strength shown by 300-M, Region II* growth rates are a factor of four lower than in 4340; the value of K_{Iscc} remaining unaffected. A similar comparison between 4340 and 300-M is shown in Fig. 2, where the two steels are compared at the same strength level, namely 4340 tempered at 300°C and 300-M tempered at 470°C. Here, Region II velocities in 300-M are almost an order of magnitude lower than in 4340, with K_{Iscc} remaining unchanged. These results confirm the initial conclusions of Carter[2] in that silicon appears to have little influence on K_{Iscc} yet results in markedly reduced growth rates for additions over 1 wt pct. The present results indicate that this increased resistance to SCC is limited to Region II velocities only.

The effect of retained austenite can be seen by comparing 300-M after quench and tempering at 470°C and after isothermally transforming at 250°C and tempering at 300°C (Fig. 2). Both structures have identical yield strengths, yet the 300M-ISO structure contains

---

*Region II refers to the plateau in growth rates, characteristically observed in SCC da/dt versus K curves, where the propagation rate is virtually independent of K. Growth rates in this region are considered to be rate-limited by the transport of chemical species, eg. H, from the environment into the region ahead of the crack tip.[5]

approximately 12 pct retained austenite, distributed as a continuous network of inter-lath films, 300-400 Å thick, within a lower bainite/tempered martensite structure (Fig. 3). SCC growth rates (in Region II) for the isothermally transformed structure are an order of magnitude lower than in the quenched and tempered structure of equivalent strength (300M-470), and nearly two orders of magnitude lower than in 4340 steel of equivalent strength. The value of K_{Iscc} again remains unchanged. Identical results for 300M-470 and 300M-ISO were obtained when tests were performed in NaCl solution (Fig. 4). A summary of SCC fracture surfaces, shown in Fig. 5, indicates that cracking is primarily along prior austenite grain boundaries; the proportion of intergranular fracture diminishes, however, as stress intensities approach K_{Ic} (ie. for $K \gtrsim 50$ MPa$\sqrt{m}$). In the 300M-ISO structure, which displayed the greatest resistance to SCC, it is noticable that there is a larger amount of ductile tearing between intergranular facets.

These results are capable of interpretation in terms of the generally accepted mechanisms[5] of SCC of martensitic high strength steels in aqueous solution, which involve a dominant role of hydrogen (ie. hydrogen embrittlement). One such mechanism[6-8] postulates that hydrogen atoms are evolved at the chemically reactive surface at the crack tip, through electrochemical reactions with the environment, and then permeate into the region of highest dilatation ahead of the crack tip where they lead to a reduction in the cohesive strength of the metal. The principal variables which affect this process are considered to be material strength, alloy composition and microstructure.[5] The enhanced

susceptibility to SCC with increase in strength for martensitic steels has been rationalized in terms of a greater solubility of hydrogen in iron resulting from an increase in hydrostatic tension.[9] The roles of composition and microstructure, however, are less clear.[10]

The present investigation has confirmed the beneficial role of silicon and demonstrated the beneficial role of retained austenite in improving resistance to environmentally-induced cracking in ultra-high strength steels. Since this improvement is in the form of lowered Region II velocities in steels of constant strength, it is felt that the roles of silicon additions and retained austenite primarily affect hydrogen permeation from the environment into the metal lattice ahead of the crack tip. Although it is not possible from such limited experiments to elucidate specific mechanisms, a few comments are worthy of note. Silicon, as an alloying addition to high strength steels, is known to enhance stability of ε-carbide to higher temperatures, and to increase the time for formation of cementite.[11] Accordingly, it has been suggested[12] that the benefical effect of silicon on SCC is related to the presence of ε-carbide acting as a hydrogen trap. Others[1,2] have postulated that silicon's role is related to its ability to prevent ε-carbide from acting as a cathodic site for hydrogen discharge. In the present study, analysis[13] of diffraction patterns of extraction replicas of polished and over-etched metallographic specimens (Fig. 6) identified the hardening carbide to be ε-carbide in the 4340-T200 and 300M-T300 structures, and cementite in the 4340-T300 and 300M-T470 structures. Since, in Table 3, 300-M structures show lower SCC growth

rates than 4340 whether or not ε-carbide is present,* it is unlikely that mechanisms[1,2,12,14] involving ε-carbide are primarily responsible for the beneficial role of silicon. However, it is observed that for either 4340 or 300-M in quenched and tempered conditions, structures hardened by ε-carbide show lower SCC velocities than *lower strength* structures hardened by cementite (cf. 4340-T300 with 4340-T200 and 300M-T470 with 300M-T300 in Table 3). Other studies[15-17] have concluded that silicon leads to a reduction in diffusivity of hydrogen in iron, and this is clearly consistent with the lower Region II (transport-limited) SCC growth rates shown by 300-M.

The most significant result of this work is the excellent SCC resistance of isothermally transformed 300-M containing retained austenite. This structure shows superior ductility and toughness to conventionally heat-treated (quenched and tempered) 300-M at equivalent strength levels (Table 1) in addition to superior environmental behavior. A plausible explanation for the markedly lower SCC growth rates can be based on the fact that hydrogen diffusivity in fcc austenite is three to four orders of magnitude lower than in bcc structures.[18] Since identical growth rates are observed in NaCl solution and distilled water, austenite does not appear to be contributing to environmental attack significantly by anodic dissolution. Furthermore, the austenite is mechanically stable in this structure[19] forming a

*300-M tempered at 470°C shows almost an order of magnitude lower growth rates than 4340 tempered at 300°C, despite its increased strength, where the only carbide present in the structure is cementite.

continuous network around laths and grain boundaries (Fig. 3), and hence any diffusion path for hydrogen ahead of the crack tip must involve transport through austenite films. Thus it is not unexpected to find the kinetics of crack growth slowed down for transport-limited Region II velocities, as experimentally observed (Fig. 2). There is also a possibility that the retained austenite films may act as "sinks" for interstitials and impurity elements[20] which may otherwise segregate to grain boundaries during heat-treatment, thereby causing enhanced environmental grain boundary attack.[21] This view is supported by the greater contribution from ductile tearing during stress corrosion cracking in the isothermally transformed structure.

The research was conducted under the auspices of the U.S. Energy Research and Development Administration through the Materials and Molecular Division of the Lawrence Berkeley Laboratory.

REFERENCES

1. C. B. Gilpin and N. A. Tiner: Corrosion, 1966, vol. 22, p.271.
2. C. S. Carter: ibid, 1969, vol. 25, p. 423.
3. R. A. McCoy and W. W. Gerberich: Met. Trans., 1972, vol. 4, p. 539.
4. J. F. Lessar and W. W. Gerberich: Met. Trans. A, 1976, vol. 7A, p. 953.
5. A. W. Thompson and I. M. Bernstein: in Advances in Corrosion Science and Technology, (M. G. Fontana and R. W. Staehle, eds.), 1977, vol. 7. Plenum. (in press).
6. L. B. Pfeil: Proc. Roy. Soc. (London), 1926, vol. 112A, p.182.
7. A. R. Troiano: Trans. ASM, 1960, vol. 52, p. 54.
8. R. A. Oriani and P. H. Josephic: Acta Met., 1974, vol. 22, p. 1065.
9. W. W. Gerberich and Y. T. Chen: Met. Trans. A, 1975, vol. 6A, p. 271.
10. I. M. Bernstein and A. W. Thompson: Int. Metall. Reviews, 1976, vol. 21, p. 269.
11. W. S. Owen: J. Iron Steel Inst., 1954, vol. 177, p. 445.
12. P. C. Hughes, I. R. Lamborn and B. B. Liebert: ibid, 1965, vol. 203, p. 728.
13. M. H. Castro Cedẽno: M. S. Thesis, University of California, Berkeley, 1977. (Lawrence Berkeley Report No. LBL-6012, May, 1977, University of California).
14. F. Nakasato and F. Terasaki: Tetsu-Tu-Hagane, 1975, vol. 61, p. 82.
15. W. W. Gerberich: in Hydrogen in Metals, (I. M. Bernstein and A. W. Thompson, eds.), 1974, p. 115. (American Society of Metals, Metals Park, Ohio, 1974).

16. A. S. Tetelman: in Fundamental Aspects of Stress Corrosion Cracking (R. W. Staehle, ed.), 1969, p. 446 (N.A.C.E., Houston, Texas, 1969).

17. E. E. Fletcher, W. E. Berry, and G. A. Elsen: ibid, 1969, p. 457.

18. J. H. Shirely, R. F. Hehemann, and A. R. Troiano: Corrosion, 1966, vol. 22, p. 253.

19. R. O. Ritchie: J. Eng. Mater. Tech., Trans. ASME Series H, 1977, vol. 99, p. 194.

20. C. W. Marschall, R. F. Heheman and A. R. Troiano: Trans. ASM, 1962, vol. 55, p. 135.

21. C. J. McMahon, Jr., C. L. Briant, and S. K. Banerji: in Fracture 1977, Proc. Fourth Int. Conf. on Fracture, (D.M.R. Taplin, ed.), Waterloo, Canada, June 1977, vol. 1, p. 363. (University of Waterloo Press, 1977).

TABLE CAPTIONS

Table I. Summary of Heat-Treatments.

Table II. Ambient Temperature Mechanical Properties of Structures Investigated.

Table III. Region II Stress Corrosion Crack Growth Rates and Values of K_{Iscc} for Structures Tested.

Table I. Summary of Heat-Treatments.

Code	Material	Heat Treatment	Prior Austenite Grain Size μm	Pct Retained Austenite*
4340-T200	4340	Austenitized at 870°C, oil quenched Tempered (1h) at 200°C	20	< 2
4340-T300	4340	Austenitized at 870°C, oil quenched Tempered (1h) at 300°C	20	< 2
300M-T300	300-M	Austenitized at 870°C, oil quenched Tempered (1h) at 300°C	20	5
300M-T470	300-M	Austenitized at 870°C, oil quenched Tempered (1h) at 470°C	20	< 2
300M-ISO	300-M	Austenitized at 870°C, isothermally held at 250°C** (1h), oil quenched Tempered (1h) at 300°C	20	10-12

*Measured using standard X-ray and magnetic saturation techniques.

**Isothermal transformation temperature (250°C) is 20 degrees C below M_s (equivalent to martempering).

Table II. Ambient temperature mechanical properties of structures investigated.

Structure	Yield Strength[1] (MPa)	U.T.S. (MPa)	Elongation[2] (pct)	K_{Ic}[3] (MPa$\sqrt{m}$)
4340-T200	1612	2087	13.5	65.9
4340-T300	1498	1755	13.0	62.7
300M-T300	1737	2006	11.9	65.1
300M-T470	1497	1683	12.1	68.9
300M-ISO	1497	1862	14.5	88.5

[1] measured using 0.2 pct offset

[2] measured on 1 inch gage length

[3] plane strain fracture toughness (valid with respect to ASTM specifications).

Table III. Region II stress corrosion crack growth rates and values of K_{Iscc} for structures tested

Structure	Region II SCC growth rate (da/dt) at K = 40 MPa$\sqrt{m}$	K_{Iscc}	Yield Strength
	(mm/sec)	(MPa$\sqrt{m}$)	(MPa)
4340-T300	1.6×10^{-2}	16.6	1498
4340-T200	6.0×10^{-3}	16.6	1612
300M-T470	2.3×10^{-3}	18.0	1497
300M-T300	1.7×10^{-3}	18.6	1737
300M-ISO	4.0×10^{-4}	18.5	1497

FIGURE CAPTIONS

Fig. 1. Variation of stress corrosion crack growth rate (da/dt) with instantaneous stress intensity (K) for 4340 and 300-M, heat-treated to their respective optimum and commercially-used tempered conditions. Tests were performed in distilled water at ambient temperature. (σ_y is the yield strength, K_{Ic} the plane strain fracture toughness and K_{Iscc} the threshold for environmentally-induced cracking).

Fig. 2. Variation of stress corrosion crack growth rate (da/dt) with instantaneous stress intensity (K) for 4340 and 300-M, heat-treated by quench and tempering and by isothermal transformation to give identical yield strength. Tests were performed in distilled water at ambient temperature.

Fig. 3. Transmission electron micrograph of 300-M, isothermally transformed at 250°C and tempered at 300°C (300M-ISO), showing distribution of retained austenite; a) bright field, b) dark field of austenite reflection, c) selected area diffraction pattern showing austenite spots and d) corresponding explanatory line drawing.

Fig. 4. Variation of stress corrosion crack growth rate (da/dt) with instantaneous stress intensity (K) for 300-M, quenched and tempered (300M-T470) and isothermally transformed (300M-ISO) to the same yield strength. Tests were performed in 3.5 wt. pct. NaCl solution at ambient temperature.

Fig. 5. Scanning electron micrographs of stress corrosion fracture surfaces in Region II at K = 35 MPa$\sqrt{m}$ for structures a) 4340 tempered at 200°C, b) 300-M tempered at 300°C, c) 4340 tempered at 300°C, d) 300-M tempered at 470°C, e) 300-M isothermally transformed at 250°C, tempered at 300°C.

Fig. 6. Typical diffraction patterns obtained from extraction carbon replicas of polished and over-etched metallographic specimens showing presence of a) ε-carbide in 300-M tempered at 300°C, and b) cementite in 300-M tempered at 470°C.

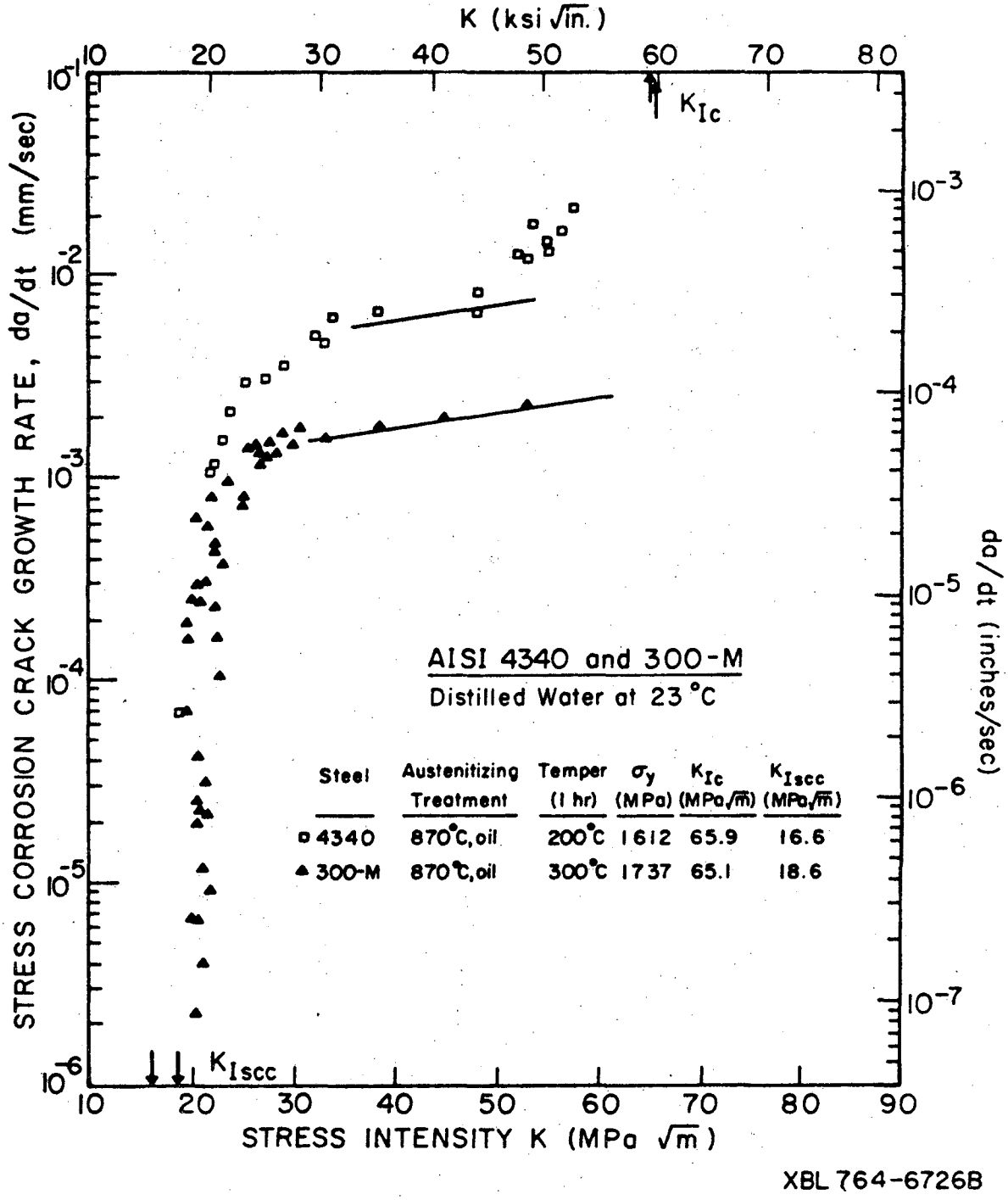

Fig. 1. Variation of stress corrosion crack growth rate (da/dt) with instantaneous stress intensity (K) for 4340 and 300-M, heat-treated to their respective optimum and commercially-used tempered conditions. Tests were performed in distilled water at ambient temperature. (σ_y is the yield strength, K_{Ic} the plane strain fracture toughness and K_{Iscc} the threshold for environmentally-induced cracking).

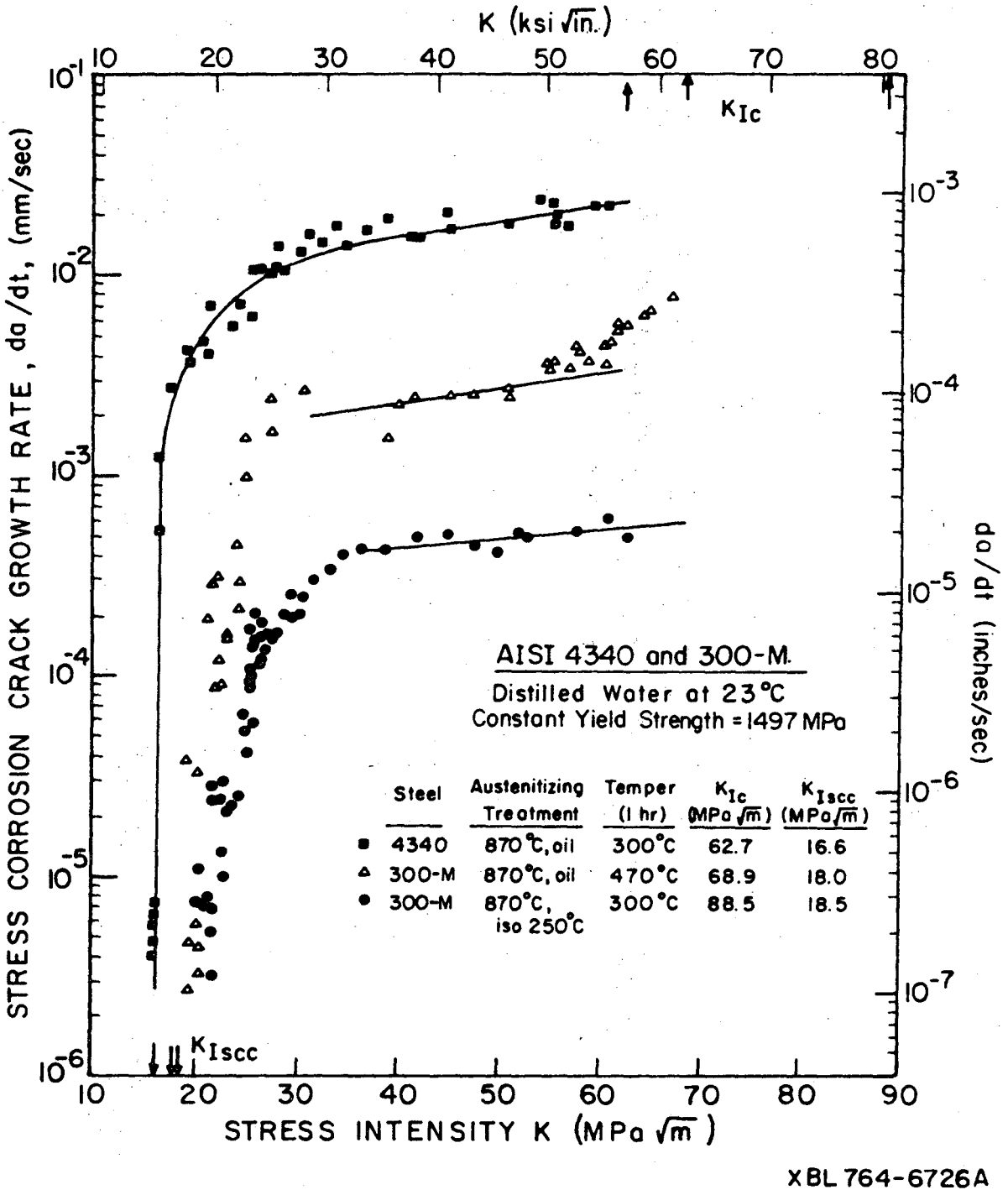

Fig. 2. Variation of stress corrosion crack growth rate (da/dt) with instantaneous stress intensity (K) for 4340 and 300-M, heat-treated by quench and tempering and by isothermal transformation to give identical yield strength. Tests were performed in distilled water at ambient temperature.

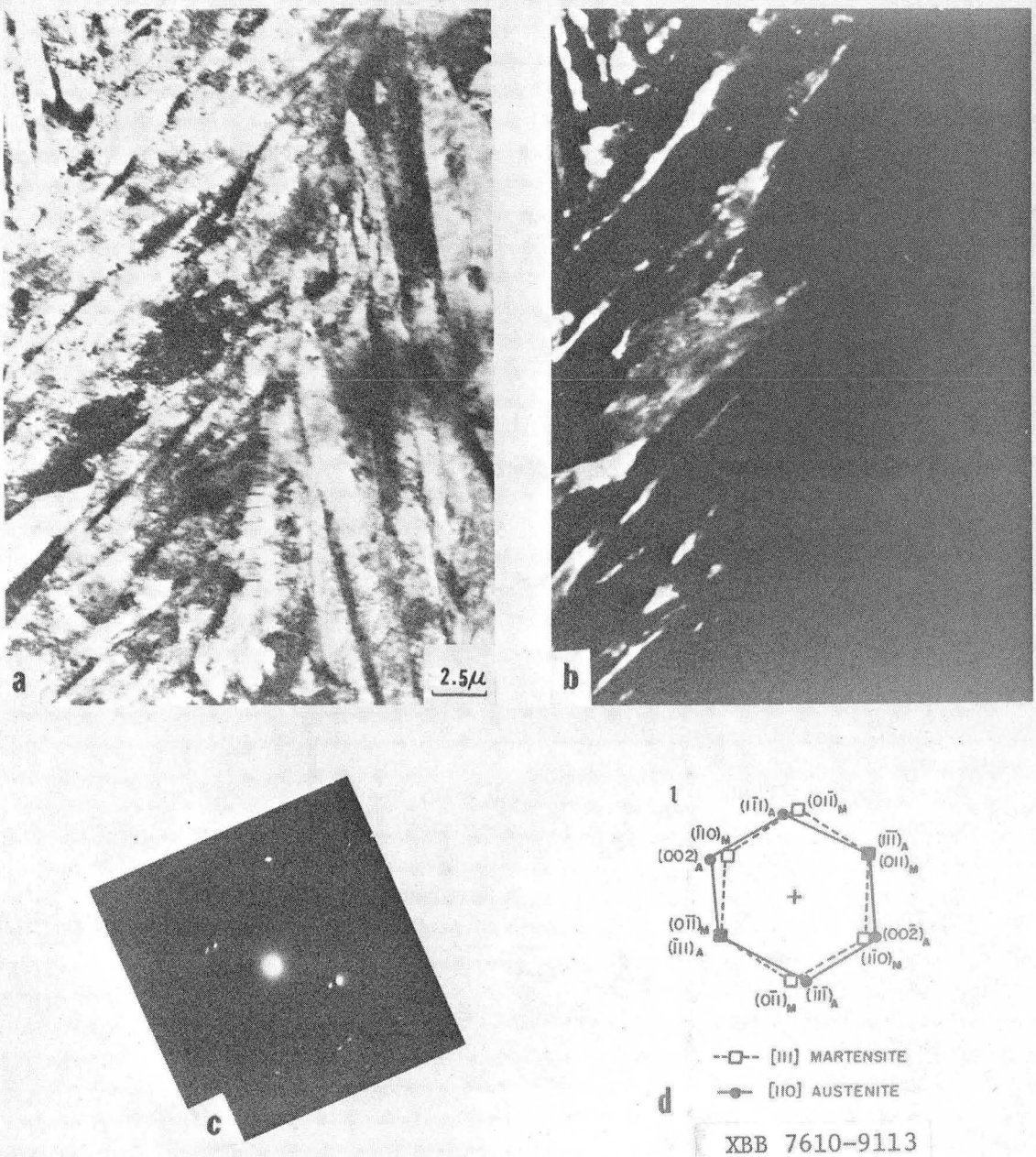

Fig. 3. Transmission electron micrograph of 300-M, isothermally transformed at 250°C and tempered at 300°C (300M-ISO), showing distribution of retained austenite; a) bright field, b) dark field of austenite reflection, c) selected area diffraction pattern showing austenite spots and d) corresponding explanatory line drawing.

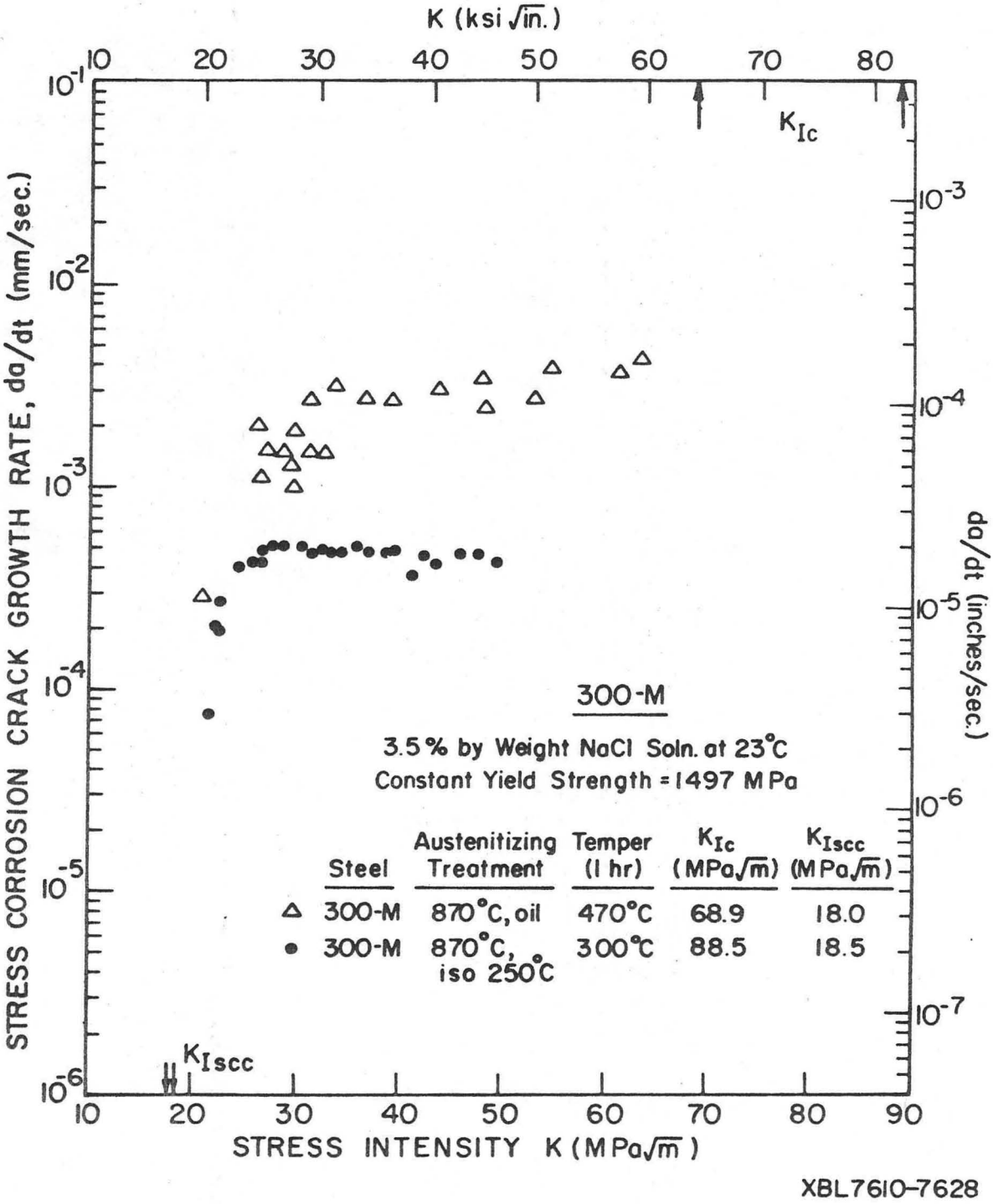

Fig. 4. Variation of stress corrosion crack growth rate (da/dt) with instantaneous stress intensity (K) for 300-M, quenched and tempered (300M-T470) and isothermally transformed (300M-ISO) to the same yield strength. Tests were performed in 3.5 wt. pct. NaCl solution at ambient temperature.

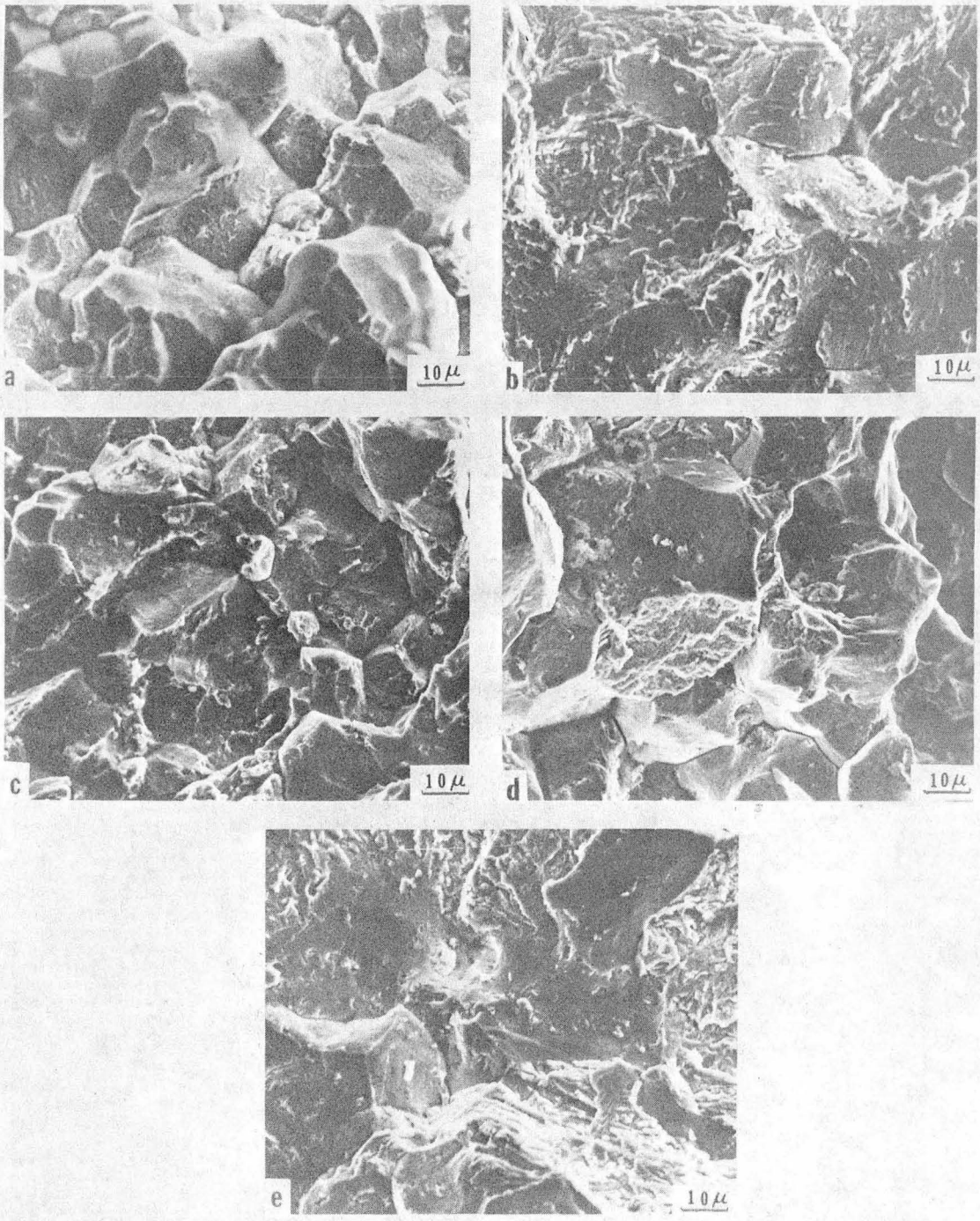

XBB 760-10108

Fig. 5. Scanning electron micrographs of stress corrosion fracture surfaces in Region II at K = 35 MPa$\sqrt{m}$ for structures a) 4340 tempered at 200°C, b) 300-M tempered at 300°C, c) 4340 tempered at 300°C, d) 300-M tempered at 470°C, e) 300-M isothermally transformed at 250°C, tempered at 300°C.

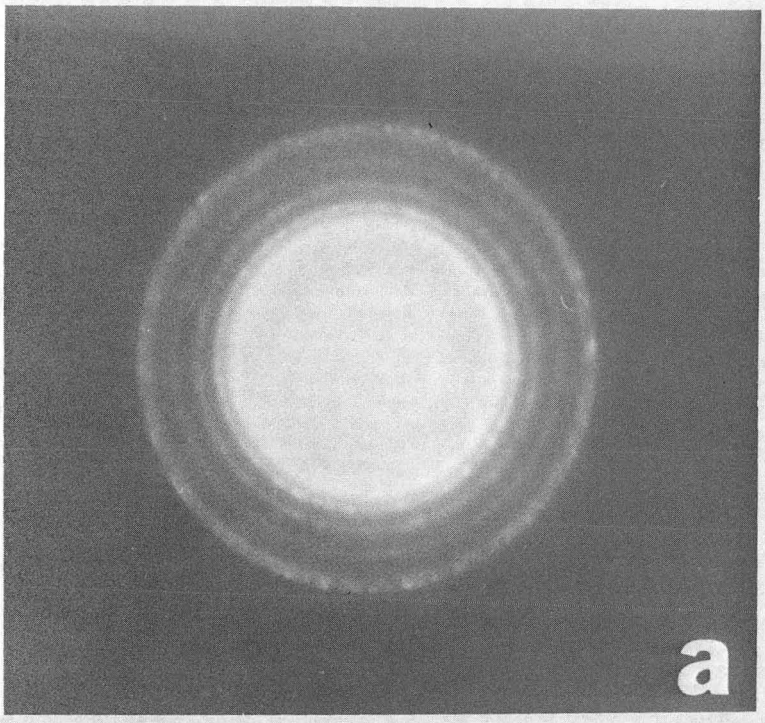

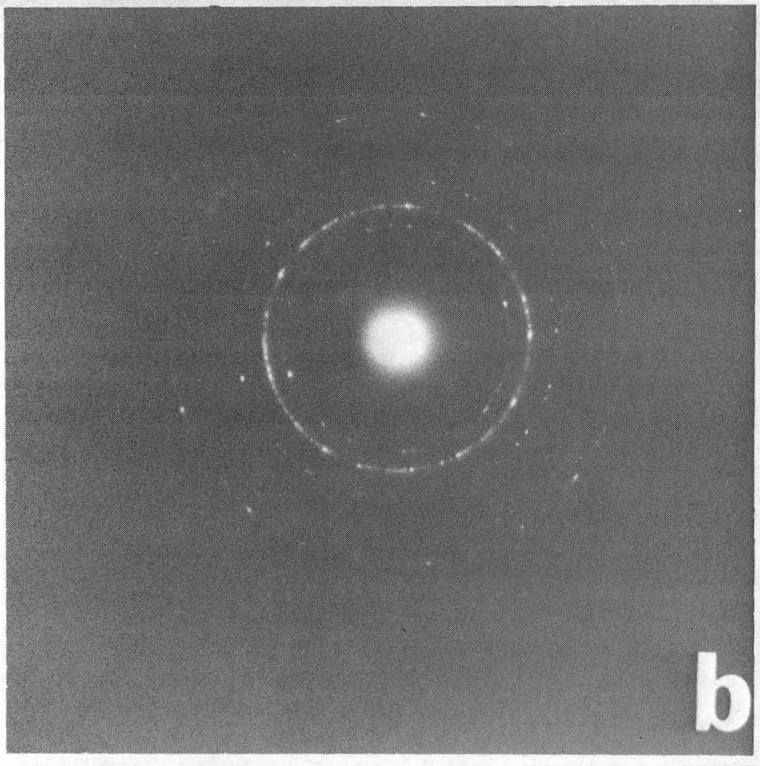

XBB 773-1686

Fig. 6. Typical diffraction patterns obtained from extraction carbon replicas of polished and over-etched metallographic specimens showing presence of a) ε-carbide in 300-M tempered at 300°C, and b) cementite in 300-M tempered at 470°C.

TECHNICAL INFORMATION DIVISION
LAWRENCE BERKELEY LABORATORY
UNIVERSITY OF CALIFORNIA
BERKELEY, CALIFORNIA 94720